Eindhoven University of Technology
Eindhoven, The Netherlands
April 20, 2023

Numerical optimization and manufacturing of a bio-based 3D structure through robotic filament winding

L.P.J. Krijnen*

*Department of the Built Environment, Structural Engineering and Design
Eindhoven University of Technology, The Netherlands
l.p.j.krijnen@student.tue.nl

Abstract

The presented work investigates the application of resin-impregnated biobased sisal rope for structural purposes. A simply supported lightweight structural element was designed to be loaded in axial compression. The element was numerically optimized to maximize buckling resistance and minimize mass and internal elastic energy. The optimized design was manufactured through robotic filament winding using biobased sisal rope, impregnated with SR InfuGreen 810 / SD 8824 epoxy resin. Robotic filament winding with bio-based materials provides opportunities for the built environment to create innovative structural elements in a fully digitized manufacturing process. Moreover, the combination of numerical optimization, innovative structural design and robotic filament winding with bio-based materials, allows to design and manufacture lightweight structures with a large degree of freedom. This can result in reduced environmental pollution caused by the traditional design and manufacturing processes of the construction sector. The manufactured fibre composite columns were after curing tested in axial compression, which resulted in a maximum compressive strength of 21.4 kN. Although the structural behaviour of the fibre composite columns was promising, further research should be conducted to conclude whether robotic filament winding with resin-impregnated sisal rope is suitable for large-scale structural purposes.

Keywords: Optimization, lightweight structures, parametric engineering, robotic filament winding, sisal fibre, biobased, axial compression, innovative structural design

1. Introduction

Ever since the beginning of the Industrial Revolution, numerous countries around the world experienced economical and industrial growth, which increased worldwide environmental pollution significantly [1]. The growing construction industry contributes to a large extent to this environmental pollution, concerning energy consumption, greenhouse gas emissions, waste generation and material depletion [2]. Moreover, the construction sector causes 36% of the energy consumption and 39% of the greenhouse gas emissions produced globally [3]. Already a third of these emissions is generated by the production process of steel and cement [4]. Considering The Netherlands, almost a quarter of the total CO_2-emissions produced during the first quartile of 2022 was generated by the built environment only [5]. Hence, the environmental contamination caused by the built environment needs to be reduced to create a healthier environment. Therefore, the Dutch government set a goal in line with the internationally established 2030 Sustainable development goals and the Paris Agreement, for the Dutch economy to be completely circular by 2050 [6].

Increasing the use of bio-based materials in the construction sector can reduce environmental pollution. Bio-based materials are composed of renewable resources, which contribute to a circular economy that aims to maximize the worth of resources and to limit the generation of waste by regenerating materials at the end of their lifecycle [7]. In addition, reusing and recycling materials reduces material depletion and lowers the amount of greenhouse gas emissions normally generated during the production process

of non-renewable materials. Consequently, the utilization of primary resources reduces, and the lifespan of existing materials extends. Nevertheless, the building industry is hesitant in implementing bio-based materials due to the lack of test results and therefore relatively unknown material properties [8]. Experimental testing with bio-based materials is required to be able to guarantee structural safety.

Furthermore, sustainability can be improved by reconsidering the structural design and manufacturing process. Traditional design methods are time and labor intensive, which involve high costs. Moreover, structural designs often get over-dimensioned due to limited accuracy and prescribed shapes and dimensions in production, which limits design freedom and the ability to optimize material use. Hence, digitizing the design process reduces time and labor intensiveness, guarantees accuracy, and allows for a higher level of design complexity and optimization processes. Consequently, using optimization processes allows for designing lightweight structures, which are minimized in mass and maximized in stiffness. Besides digitizing the design process, robotics can be used to automate the manufacturing process as well, which reduces labor intensiveness and allows to manufacture complex structures with a large degree of freedom.

The aim of this research is to design an optimized three-dimensional lightweight structure to transfer an axial compressive force, and to manufacture this structure by robotic filament winding using resin impregnated bio-based sisal rope. The simply supported structural element has a prescribed height of one meter and should be able to be placed in a spaceframe. This research is part of the Innovative Structural Engineering and Design (ISD) field and focuses on minimizing material use and integrating architectural and structural design. The research question is formulated as follows:

'How can an axially loaded, bio-based, three-dimensional structure be manufactured by robotic filament winding and be optimized through numerical optimization?'

Figure 1 provides a schematized representation of the research question, where the dotted line represents the optimized filament-winded structure to be designed. Robotic filament winding with bio-based materials provides opportunities for the built environment to create innovative structural elements in a fully digitized manufacturing process. Moreover, the combination of numerical optimization, innovative structural design and robotic filament winding with bio-based materials, allows to design and manufacture lightweight structures with a large degree of freedom. As a result, environmental pollution caused by the traditional design and manufacturing processes of the construction sector, can be reduced.

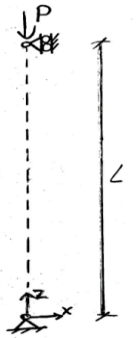

Figure 1 Schematization research question

2. Literature study

The architect and professor Achim Menges designed in corporation with the Institute for Computational Design (ICD) and the Institute of Building Structures and Structural Design (ITKE) at the University of Stuttgart several robotically fabricated lightweight composite structures. As a result, three items are highlighted which are of importance to design robotically filament-winded structures. First, robotic filament winding is a tension-driven process with fibers spanning between anchor points or contact points with other fibers. Since fibers are stronger in tension and prone to buckle in compression, the fiber use in tension should be maximized at all times. Secondly, the fiber span should be reduced to increase the buckling strength, which can be done using fiber interlocking. Thirdly, adding surface curvature perpendicular to the stress direction increases the buckling strength. Furthermore, a robotic winding path is defined by a single start and end point, which implies that horizontal tension rings to increase the strength could not be manufactured since they interrupt the winding path [9].

A study on lightweight structures conducted by Beukers & Hite [10] also shows that nature can be used as inspiration for structural design, since nature uses a minimum amount of energy. This principle can be seen in the shape of a tree, which is based on the history of loading. Therefore, lightweight structures should be designed based on the flow of forces to minimize energy and material use.

The governing failure mechanism of slender structures loaded in axial compression is buckling [11]. Buckling can be seen as a sudden failure of the structural member, occurring before the ultimate compressive stresses in the material are reached [12]. The German-Swiss mathematician Euler analyzed buckling in the 18th century and established several Euler conditions to predict the critical load. Figure 2a shows the buckling shape and formula to predict the critical load for a simply supported column loaded in axial compression [10]. Since the length of the pin-ended column is set to one meter, the critical length will also be one meter. This in turn means that the critical load is only depending on 2 variables: the Young's modulus of the material and the moment of inertia of the cross-section. Moreover, the moment of inertia is the only parameter that can be affected by the column design. An increased moment of inertia results in a directly proportional increase of the critical load. The moment of inertia can be increased by distributing the material as far from the principal axes of the column as possible, while the wall thickness remains thick enough to prevent local buckling [12]. Consequently, columns with a tubular cross-section result in a higher critical load and therefore buckling resistance.

In line with this research, Pawlyn [13] conducted research on biomimicry in architecture which concluded that a convex-shaped column with a circular hollow cross-section has the same stiffness as a column with a solid squared cross-section, while only using 14% of the material. Placing material according to the flow of forces results in shape and material optimization. Therefore, a typology optimization and FEM-analysis are conducted to analyze the flow of forces. From Figure 2b to 2d it can be seen that a convex-shaped structure is created to travel the applied force to the support. Furthermore, the cross-sectional area of the structure increases towards the middle of the column, where the highest resistance against buckling is required. These analyses verify the research conducted by Beukers & Hinte [10] and Pawlyn [13]. As a result of these findings, the Grasshopper script should be able to generate a convex-shaped column with a tubular circular cross-section.

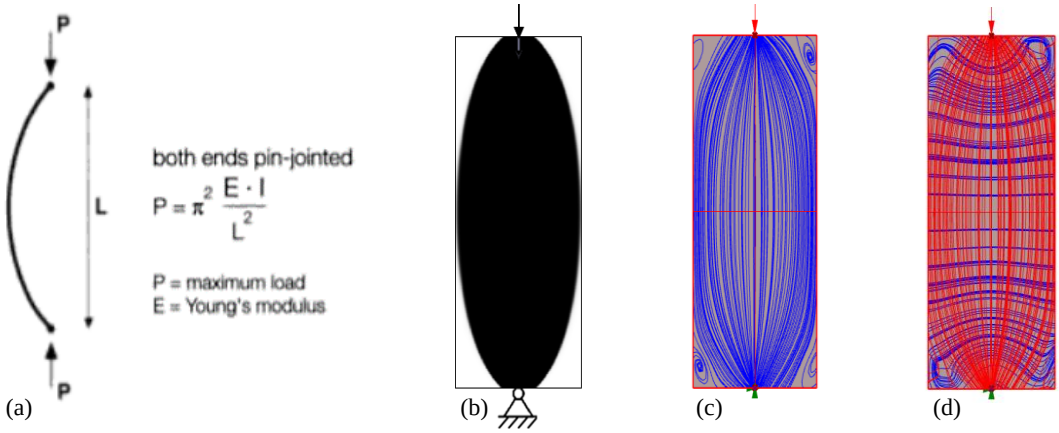

Figure 2 (a) Euler buckling shape and formula to predict critical load [10] (b) Typology optimization (c) Flow of forces (d) Principle stresses

3. Materialization

The structural element is manufactured of biobased sisal rope impregnated with SR InfuGreen 810 / SD 8824 epoxy resin. Sisal rope is made from natural sisal fibre, derived from the leaves of the Agave sisalana plant. The fibres are renewable, biodegradable, and abundantly available [14]. The epoxy resin SR InfuGreen 810 has with an average carbon green content of 38% also a relatively low environmental impact [15]. Furthermore, the two-component epoxy system has a relatively low viscosity at ambient

temperature, which enhances the workability during winding. Natural fibres such as sisal fibre characterize unidirectional properties and a high tensile strength, which is why they are mostly used for structural purposes such as ropes and reinforcement. Furthermore, due to their low density and high strength-to-weight ratio, natural fibers create opportunities for the built environment to design and manufacture lightweight structures [16]. A large variety of natural fibers is therefore also used for robotic filament winding. Since natural fibres derive from nature, the cross-section throughout the fibre length and mechanical properties can vary strongly due to the growth location and environmental conditions during growth such as rainfall [17]. Natural fibres characterize a high moisture absorption compared to glass and carbon fibres, which is why the latter can strongly influence mechanical properties [14]. Furthermore, the mechanical properties of woven fibers highly depend on the yarn twist, fiber orientation and fiber cohesion [18]. As a result, the mechanical properties of natural sisal fibre vary significantly. Therefore, previous graduates from TU/e conducted tensile tests with the same material as will be used for this research, namely, 4 mm three-stand sisal rope impregnated with SR InfuGreen 810 / SD 8824 epoxy resin [19]. The average tensile strength of 100 MPa and Young's modulus of 4000 MPa resulting from these tests are used as a guideline for the numerical model. The results of the numerical model are compared to test results in a later stage.

4. Numerical optimization

The numerical optimization is conducted in Rhinoceros through a script written in Grasshopper, and is divided into two parts. The first part defines the geometrical design of the column, which can be defined by six geometrical parameters. These parameters allow the script to create either a straight, concave or convex-shaped column with an x amount of vertical and diagonal lines. Also, the amount and angle of the diagonal lines can be set by these parameters. The structural analysis of the model is done using the parametric, structural engineering tool Karamba3D. Since there are three fitness function values to be optimized, the Multi-Objective Evolutionary Optimization plug-in Octopus is used which allows solving for multiple optimization objectives at once. While changing the geometrical parameters, Octopus searches for an optimized structure that is minimized in mass and internal elastic energy, and maximized in resistance against buckling. This results in a range of trade-off solutions between the extremes of each goal, visualized in a three-dimensional graph (Figure 3a) [20]. The solution closest to the origin is found the most optimal design for the defined fitness function values. This design is visualized in Figure 3b.

The second part of the numerical optimization is an iterative sizing optimization to optimize the number of ropes for each line. This iterative process distributes the material based on the strain energy. First, the strain energy is calculated for each line based on Formula 1.

$$U_i = \frac{\sigma_i^2 * V_i}{2 * E} \tag{1}$$

Secondly, the strain ratio is calculated by dividing the strain energy per line U_i by the total strain energy. This strain ratio is used to calculate the new cross-sectional area per line $A_{i,new}$. To prevent the iterative loop from taking too big steps per iteration, the constraint is set that the new cross-sectional area $A_{i,new}$ may not differ more dan 10% compared to the previous cross-sectional area A_i. Based on the new cross-sectional areas, the new line volumes are calculated and Karamba3D is used to structurally analyze and calculate the new model. This calculation results in new maximum stress values per line $\sigma_{i,new}$. After this, one iteration is completed and the loop can run again.

As a result, the amount of ropes increases for highly stressed lines and decreases for less stressed lines (Figures 3c and 3d). Table 1 provides the result of the sizing optimization after ten iterations. The buckling load factor (BLFacs) increased, which is the factor by which the applied force can be multiplied before buckling occurs. Furthermore, the elastic energy change and mass reduced, which implies that the stiffness of the column increased while using less material. From Figure 3e, it can be observed that the structural analysis of the final optimized design refers to the earlier conducted principle stress analysis. Consequently, the optimized design is based on the flow of forces.

Table 1 Structural analysis before and after sizing optimization

	Mass [kg]	Elastic energy change [kNm]	BLFacs [-]	Max displace-ment [cm]	Max comp. stress [MPa]	Max tensile stress [MPa]
Before sizing optimization	2.79	2.23 x 10^-4	35.05	0.045	3.94	1.80
After sizing optimization	2.46	1.52 x 10^-4	39.10	0.030	2.91	1.58
Difference	-11.83%	-31.84%	+11.55%	-33.33%	-26.14%	-12.22%

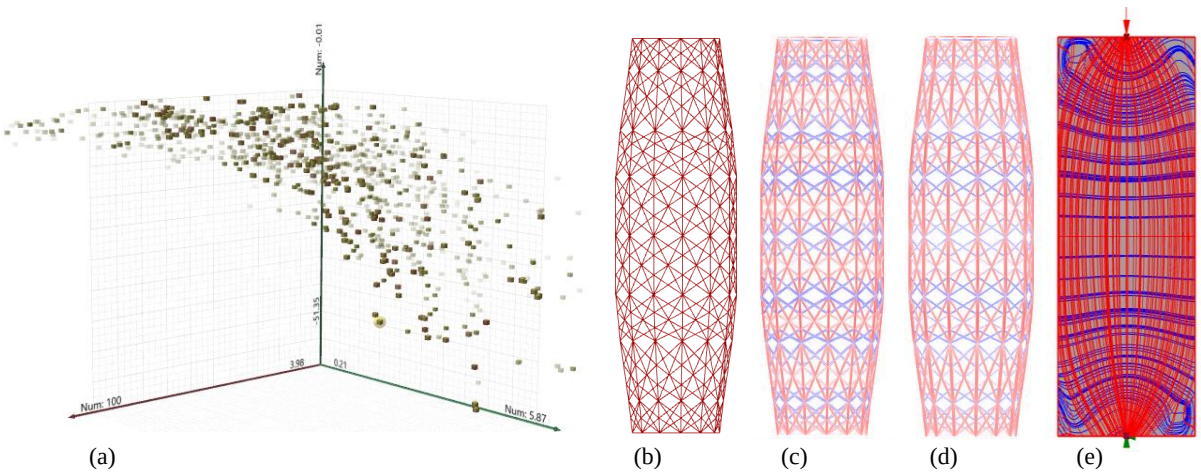

(a) (b) (c) (d) (e)

Figure 3 (a) Result Octopus optimization (b) Optimized design (c) Structural analysis optmized design before sizing optmization (d) Structural analysis after sizing optimization (e) Principle stress analysis

5. Robotic filament winding

5.1. Eulerian winding path

To manufacture the structure by filament winding, an Eulerian path is defined to be able to wind the column in one continuous session. To define this path, it should be taken into account that the vertical lines should be winded before the diagonals. Consequently, if the diagonals would be winded first, there are limited contact point between the verticals and diagonals, which decreases the strength of the column. By winding the diagonals around the verticals, the amount of contact points increases and the fibre span reduces, which increases the buckling resistance of the column [9]. The Leafvein plug-in is used to define an Eulerian path for different layers to control the winding sequence. This results in a list of points, defining the robot path with a single start and end point.

5.2. Filament winding

The optimized structural element will be manufactured through robotic filament winding: a manufacturing process where resin-impregnated uncured fibres are sequentially wrapped around a minimal formwork, following a given path. Filament winding is a tension driven process where fibers span between anchor points or contact points with other fibres. Since the numerically optimized design resulted in a slightly convex-shaped column, a non-structural formwok is required to wind the impregnated sisal rope around. This formwork is connected to a moveable work object, which communicates with the robot and ensures that the formwork is rotated in correct position, while the robot only moves from left to right along the column length. The robot used for manufacturing is ABB IRB 1200-5/0.9, which is available in the Structural Engineering and Design (SED) lab at TU/e. The location of the robot and moveable work object are calibrated, which provides the input for Robot

Components. The points resulting from the Eulerian path are moved outwards to prevent collision between the formwork and the robot. Furthermore, the planes of the target points are aligned with the plane orientations of the robot and moveable work object. This data is combined, resulting in a RAPID Program and System Module. The Program Module script, also known as the MainModule, defines robot movements. The System Module script, or BASE-code, defines the robot head orientation based on the applied end effector. The RAPID-code can be loaded into Robot Studio for manufacturing.

To allow the robot to interact with the environment, an end effector should be detached to the robot arm, which is able to guide the resin-impregnated rope to specific target points. This end effector is made from aluminium and steel elements, as can be seen in Figure 4. Since aluminium and steel can bond with epoxy resin, a rubber is placed in the steel tube which prevents the tube from being damaged by the resin. Furthermore, the rubber increases the radius of the curve. This decreases the stresses on the end effector, ensures smoother winding, and prevents the rope from shearing sharply along the steel tube.

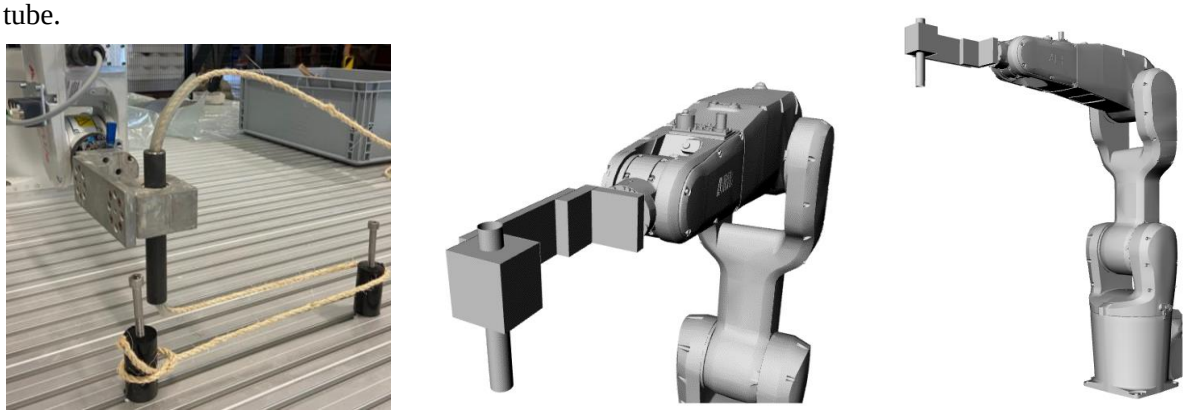

Figure 4 End effector connected to ABB IRB 1200-5/0.9 robot

Before the rope reaches the end effector, it needs to be unwound from the spool, impregnated with epoxy resin, and pre-tensioned. This total process is visualized in

Figure 5. The required sisal rope length to wind one column is 175.4 meters. It is preferable to wind the column in one continuous session. Therefore, sisal rope spools of 220 meters are used for manufacturing. The rope is unwound from the spool and guided through a steel eye to the resin bath, where the rope is fully impregnated over 200 mm. After the resin bath, the rope passes through a rubber with a narrow circular opening to release redundant resin and create tension on the rope. The tensioned and impregnated rope is guided through another steel eye to the robot end effector which winds the rope around the formwork according to the generated RAPID-code.

Figure 5 Filament winding setup

5.3. Formwork design

The non-structural formwork required for manufacturing should be able to be removed after the structure is cured. Figure 6 shows the final formwork design, made of MDF elements placed on a threaded rod. To ensure the formwork can be removed through the column ends, the base circle of the elements has a radius of 92 mm. Fork elements are bolted with small M4 bolts to these circular base plates. During manufacturing, the rope will be placed in these fork elements where the fibres are pushed against each other to create bonding. The contact area between fibres must be maximized to maximize the bonding strength. Furthermore, the elements ensure the rope stays in place. For the formwork ends, aluminium end nodes were designed for manufacturing, consisting of a ring and base plate. The aluminium ring features 13 M6 bolts, to wind the sisal rope around. The base plate can be placed in the ring, and can be used to connect the ring to the threaded rod by clamping it within two nuts. The two aluminium elements are connected by six M6 bolts. After curing, the fork elements will be broken off and these six bolts can be removed to remove the formwork through the aluminium ring at the column end. The aluminium end nodes and MDF elements are placed on a threaded rod, which is manually connected to the rotation table.

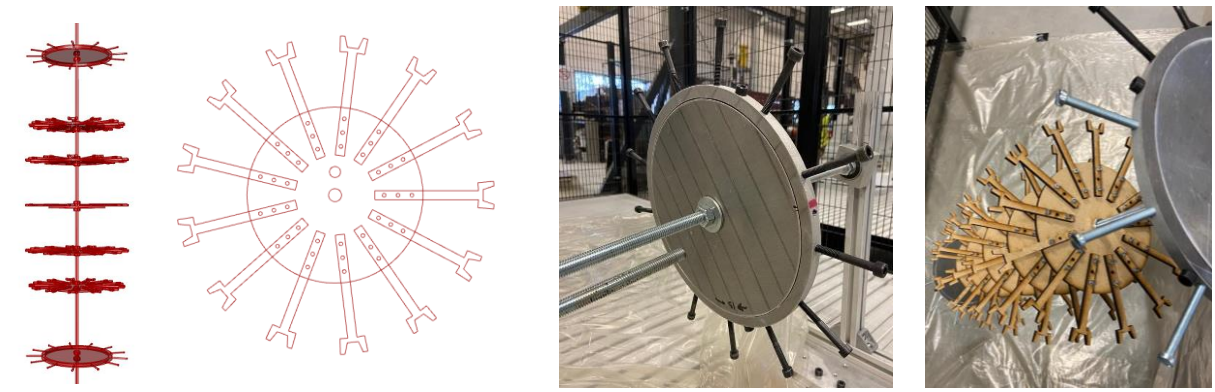

Figure 6 Final formwork design

5.4. Manufacturing

In total, four columns are manufactured (Figure 7), one of which was not fully finished due to the occurrence of a robot error during the manufacturing process. After manufacturing, the columns are stored in a climate room for a maximum of 20 hours at ambient temperature and 60% RH, after which they are post-cured for eight hours at an elevated temperature of 40 degrees Celsius. After curing, the internal formwork is removed and small column imperfections such as skewing were noticed, caused by the manually attached formwork. Furthermore, some columns seemed to have a sticky waxy film over the sisal rope. This phenomenon, called amine blush, can occur when the hardener of the two-component epoxy resin reacts with moisture and carbon dioxide [21].

Figure 7 Four fibre composite columns manufactured

6. End node

The column is designed as a simply supported column, optimized for axial compression. Furthermore, the column should be able to be placed in a spaceframe. Therefore, an end node is designed to connect the column to a bolt ball node. This connection should be able to transfer the axial compressive force to the column. Figure 8 visualizes the end node design. A cone is placed at both column ends, to create a small bolt-ball node where multiple columns can be connected to. The top of the cone can be bolted to the bolt ball node by placing a sleeve over the high-strength bolt. The sleeve and bolt are connected via a dowel pin, which allows to tighten the bolt to the bolt ball.

To ensure equal force distribution and limit local effects, the inequalities of the rope should be equalized before connecting the end cone. This can be done by casting a thin layer of plaster over the sisal rope at the column ends, indicated by the red hatched area in Figure 8a. After the plaster is hardened, the U-shaped cone end can be placed over the equalized column ends. The cone is connected to the column by 13 bolts, using the bolt holes created during manufacturing. Figure 9 visualizes a final spaceframe connection and design.

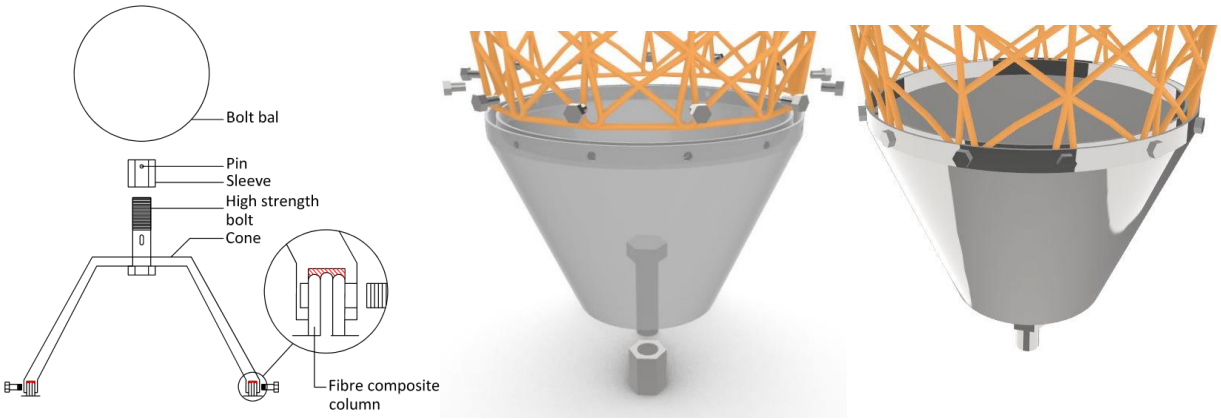

(a) (b) (c)

Figure 8 End node design

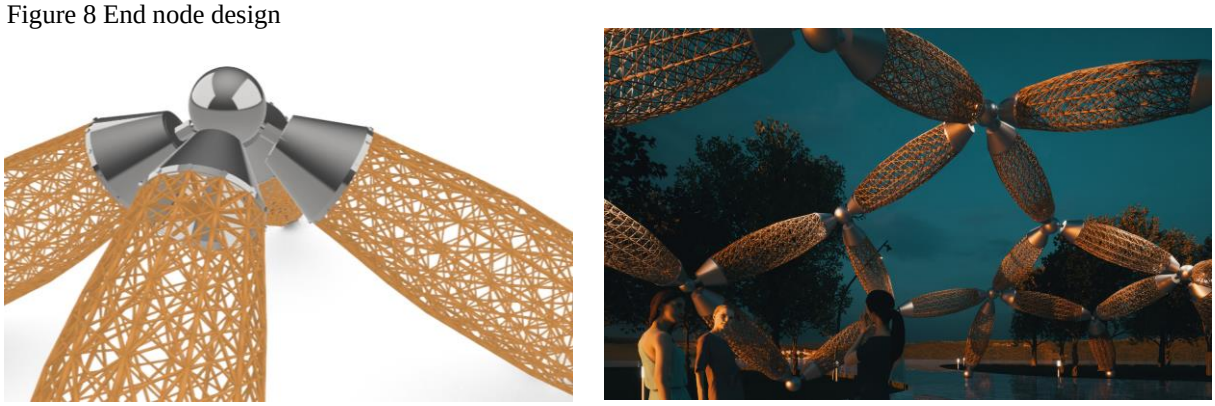

Figure 9 Visualization spaceframe connection and design

6. Axial compression tests

The four fibre composite columns are tested in axial compression in the compression testing machine at the SED lab of TU/e. The columns should be simply supported. Therefore, the column must be free to rotate at its supports, but fixed to translate. Figure 10a shows the test setup for the first axial compression test of column 1. The aluminium end nodes used during manufacturing were not removed during this test. To prevent the aluminium from being pushed into the structure, a styrofoam ring of 50 mm was placed on top of the sisal rope. Furthermore, this foam ring should equalize rope inequalities to prevent local effects. A spherical hinge was placed at the top. A steel plate is connected to this hinge, which

covers the column end and distributes the axial compressive point load over the column. At the bottom, the column was placed on a 50 mm foam ring only. This ring allows some rotation and equalizes the rope inequalities.

After testing the first column, it was discussed that the foam ring at the bottom did not allow enough rotation to mimic a pinned connection. Therefore, for the second to fourth column, a spherical hinge was placed at the top and bottom of the structural element (Figure 10b). Furthermore, the aluminium elements at the column ends should not contribute to the axial compression tests. The aim of the compression tests was to analyze the structural behaviour of the fibre composite columns. Therefore, the aluminium elements were removed after the first test. To equalize rope inequalities and prevent local effects, styrofoam plates of 20 mm were placed at both column ends.

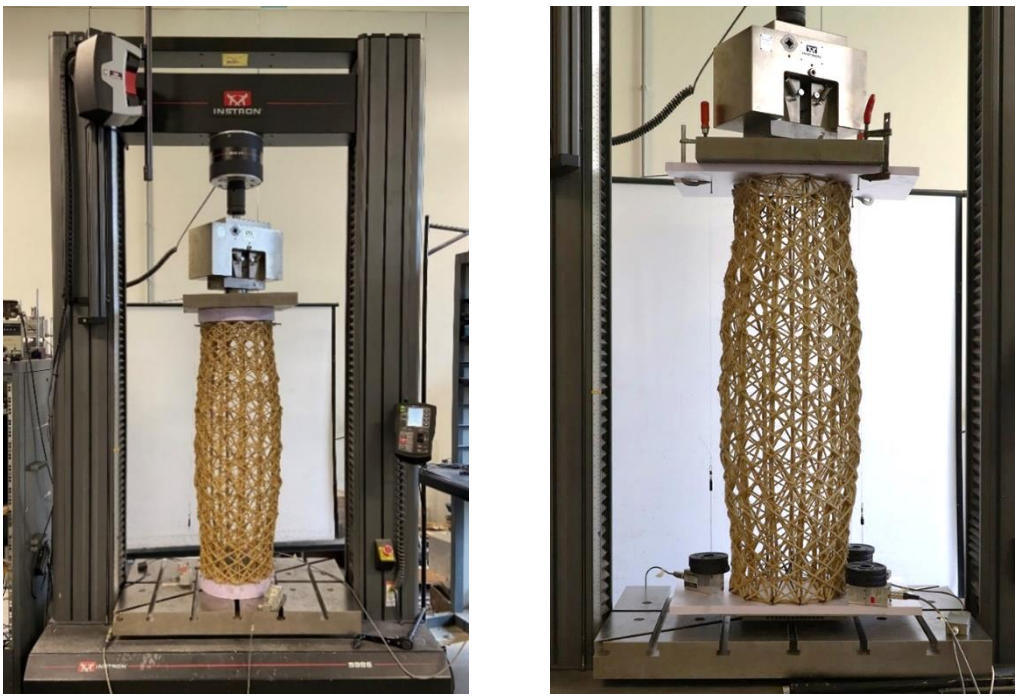

(a) (b)

Figure 10 Test setup axial compression tests for (a) column 1 and (b) column 2 to 4

For each test, three draw wire sensors were placed to measure the vertical displacement of the columns. In the first test, these sensors were connected to the bolts every 120 degrees. After removing the aluminium elements at the column ends, these sensors were connected to the steel plate in test 1b. For columns two to four, the sensors were placed between the styrofoam plates as can be seen in Figure 10b. The axial compression tests result in a force-displacement diagram incorporating the vertical displacement of the draw wire sensors and the bench displacement.

7. Results

Figure 11 provides a force-displacement diagram of the four columns combined. Up to 5 kN, the four columns show similar behaviour. After this point, the stiffness of the second column starts to decrease. This column was however not fully finished due to the occurrence of a robot error during the manufacturing process. Columns 1, 3 and 4 show similar behaviour up to approximately 20 mm displacement, which is caused by the settlement of the ropes in the styrofoam. After this point, the stiffness seems to decrease for the three columns. This is however not caused by a decreased column stiffness, but by the styrofoam being completely squashed. For column 1, this phase lasts until a

displacement of approximately 90 mm is measured. For columns 3 and 4, this phase lasts up to 30 mm displacement. This difference can be explained by the fact that the first column had a total styrofoam plate thickness of 100 mm, which was only 40 mm for columns 3 and 4. After the styrofoam is fully squashed, the columns show a similar stiffness as at the beginning of the tests. For the first column, this can be seen by the result of test 1b. In this phase, the force increases strongly with limited deformation until the maximum force is reached. After this point, the sisal rope buckles locally at the top of the columns, leading to a drop in the force-displacement graphs.

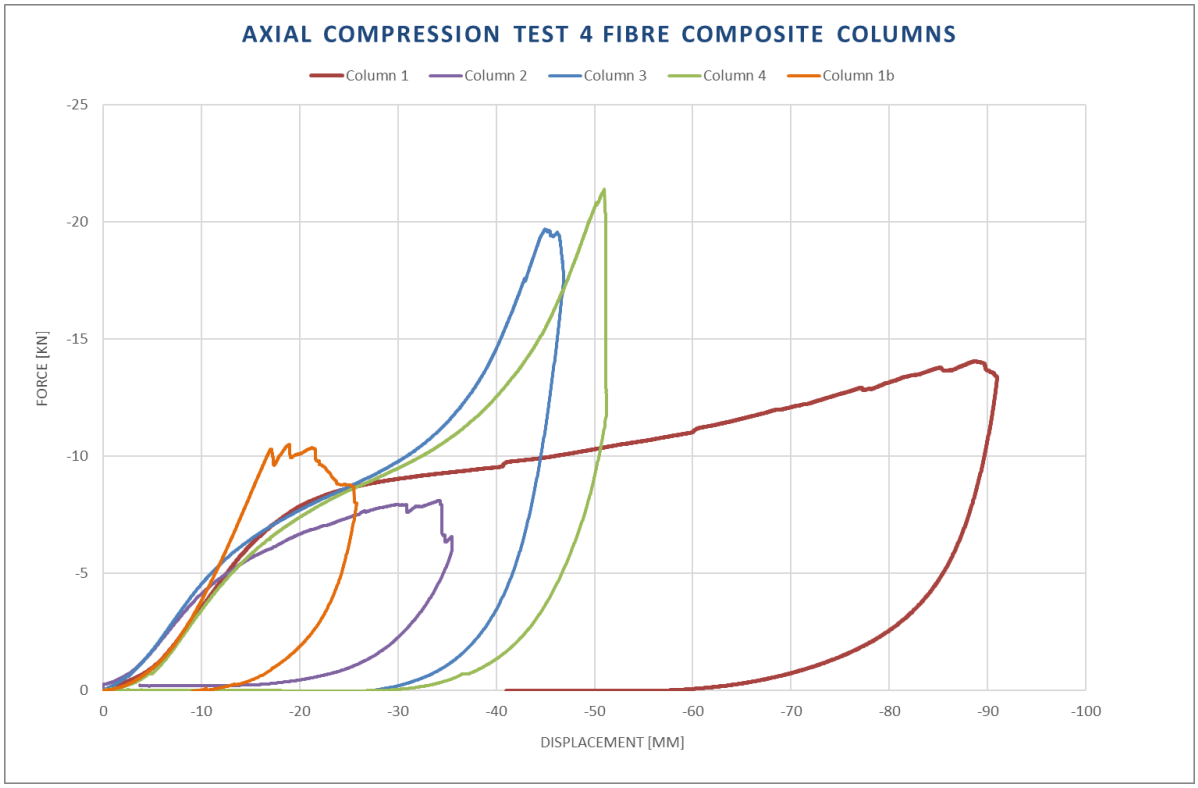

Figure 11 Force-displacement diagram of four fibre composite columns tested in axial compression

Table 2 Test results axial compression tests

Column	Max compressive force reached	Max force in numerical model	Factor difference	Failure mechanism
1	14.06 kN	39.10 kN	2.78	Local buckling of verticals at column top
2	8.11 kN	7.08 kN	0.87	Local buckling of verticals at column top
3	19.68 kN	39.10 kN	1.99	Local buckling of verticals at column top
4	21.40 kN	39.10 kN	1.83	Local buckling of verticals at column top

Figure 13 shows the visible local buckling of the sisal rope at the top of the columns after testing. During testing it could be observed that after the styrofoam plates were fully squashed, the gap size at the location where the bolts used to be enlarged at the top, resulting in multiple vertical winded ropes to detach from the structure and buckle locally. This phenomenon is explained in Figure 12.

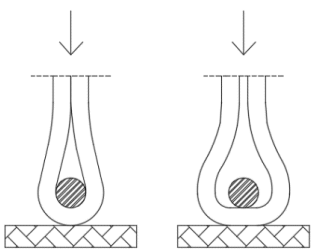

Figure 12 Local bucking sisal rope at location bolt hole

Figure 13 Visible local buckling of the sisal rope after testing

8. Discussion

It can be discussed why local buckling of the sisal rope first occurs at the top of all columns, and not at both column ends at the same time. After manufacturing the columns, the epoxy resin still had a relatively low viscosity when placed in the climate room. The columns were placed vertically against the wall of the climate room. This caused the fluent resin to leak a bit, resulting in more resin at the bottom of the column, which was visible on the aluminium bottom plate as well. The columns were tested in the same vertical position as they were cured. An increased amount of epoxy resin can result in increased strength and bonding conditions, due to which the ropes are less likely to detach and buckle. If the columns were cured rotating in a horizontal position, failure of the columns would probably occur more symmetrical.

From Table 2, an average factor difference of 1.87 is found between the test and numerical results for the buckling load. This difference can be caused by a number of factors. First, in the numerical optimization, Karamba3D assumes perfect bonding between all ropes crossing each other. In reality, the contact area between the vertical and diagonal ropes is less, since the fibres are sequentially wrapped. This results in decreased bonding conditions, which can cause local buckling to occur before the maximum force calculated by the numerical model is reached.

Secondly, since natural fibres derive from nature, the cross-section throughout the fibre length and the mechanical properties can vary strongly due to the growth location and environmental conditions. Additionally, mechanical properties of woven fibres highly depend on the yarn twist, fibre orientation, and fibre-to-fibre cohesion. All of these factors could not be controlled for the manufactured columns.

Thirdly, moisture and relative humidity can influence the strength of the composite material. The technical datasheet of the two-component epoxy system provided no prescriptions regarding the dimensions of a storage room or the relative humidity in it. The only prescription was that a minimum temperature of 20 degrees Celsius had to be guaranteed while the columns were stored before post-curing. The only location where this could be ensured was the climate room in the SED lab with an RH of 60%. After the columns were stored for a maximum of 20 hours, the columns felt somewhat sticky already, which possibly indicated that the resin started to cure. After post-curing at 40 degrees Celsius, the columns still felt somewhat sticky. The waxy film over the sisal rope, amine blush, is possibly caused by the hardener of the two-component epoxy system reacting with the carbon dioxide and moisture in the air while stored in the climate room for 20 hours. Amine blush can affect the mechanical properties of the material, which may have affected the compressive strength of the columns.

8. Conclusion

The aim of this research project was to design an optimized three-dimensional lightweight structure to transfer an axial compressive force, and to manufacture this structure by robotic filament winding of resin-impregnated bio-based sisal rope. The one meter heigh structural element should be simply supported and able to be placed in a spaceframe, for which an end node is designed.

The research was started by conducting a literature study into robotic filament winding, lightweight structures, and axially loaded simply supported columns. To create a lightweight structure, material should be placed according to the flow of forces. The flow of forces and principle stresses were studied by a FEM-analysis. Moreover, it was found that buckling is the governing failure mechanism for slender structures loaded in axial compression. From this study, the three optimization goals were found, namely, minimize mass and internal elastic energy, and maximize resistance against buckling. Furthermore, it was found which geometrical shapes the optimization script should be able to generate, resulting in a set of parameters. These parameters and optimization goals are used to set up the numerical model in the parametric modelling software Rhinoceros, through a script written in Grasshopper. While changing geometrical parameters, the script searches for an optimized lightweight structure to take an axial compressive force. After the optimized geometrical design was found, an iterative sizing optimization was conducted. This iterative process distributes the material based on the strain energy. As a result, the amount of ropes increases for highly stressed lines and decreases for less stressed lines, resulting in a final design with a slightly decreased mass and an increased stiffness and buckling resistance.

After finding the optimized column design, a winding path was determined which allowed the column to be manufactured in one continuous winding session. Robot Components was used to combine all actions with the moveable work object and specified robot. This resulted in RAPID-code, which was loaded into Robot Studio to simulate the complete winding path and manufacture the structure.

For manufacturing, a non-structural formwork had to be designed which should be able to be removed after the structure was cured. Through trial and error, a final formwork design was made of MDF elements placed on a threaded rod, which could manually be connected to the rotation table. Furthermore, the design of the robot end effector was adapted several times to improve the winding process. The final structure was manufactured using a 4 mm three-strand sisal rope, impregnated with SR InfuGreen 810 epoxy resin and SD 8824 hardener. This material was chosen to continue on previously conducted studies at TU/e. The sisal rope was unwound from the spool and guided through a resin bath, after which the impregnated rope was tensioned by a rubber and directed to the end effector. The full filament winding process was tested multiple times before final manufacturing.

In total, four columns were manufactured, one of which was not fully finished due to the occurrence of a robot error during the manufacturing process. The columns were stored in a climate room for a maximum of 20 hours at ambient temperature, after which they were post-cured for eight hours at an elevated temperature of 40 degrees Celsius. After curing, the internal formwork was removed and small column imperfections such as skewing were noticed, caused by the manually attached formwork. Furthermore, some columns felt somewhat sticky as a result of the hardener reacting with carbon dioxide and moisture while being stored at ambient temperature before post-curing.

The cured fibre composite columns were tested in axial compression in the compression testing machine, after which an average factor difference of 1.87 was found between the test and numerical results for the buckling factor. The governing failure mechanism of the axial compression tests was local buckling. Since the filament-winded column is not one single element but an interaction of multiple elements, it is more likely that local buckling of the sisal rope occurs before global buckling of the column occurs.

After this research, it can be concluded that it is feasible to manufacture a numerically optimized column design through robotic filament winding using biobased sisal rope. Besides some imperfections caused by the manually attached formwork and the curing process, the structural behaviour of the winded columns was promising. Further research should be conducted into the curing process of the epoxy resin and the formwork design to improve the process and conclude whether robotic filament winding with sisal rope is suitable for large-scale structural purposes.

Acknowledgements

The author acknowledges the graduation committee for its guidance throughout the project. Special thanks to Ir. A.P.H.W. Habraken for his enthusiasm towards the project, and for his weekly feedback which was very helpful. Ir. M.T. Ferguson especially for sharing his knowledge regarding robots, and providing help during the test manufacturing phase. Dr. Ir. S.P.G. Moonen for his commitment, and for sharing his knowledge regarding biobased materials and robotic filament winding reference projects. Furthermore, the author acknowledges the staff from the SED lab of Eindhoven University of Technology for their support and involvement throughout the manufacturing and test phase of the project. Lastly, a special thanks to colleague students. V.B. Staat for his commitment throughout the project, and for brainstorming together. L.M.J. Roex, D. Jansen and R.T. Damoiseaux for their helping hands during the winding process.

References

[1] Ahmed, F. (2022, January 7). *The environmental impact of industrialization and foreign direct investment: empirical evidence from Asia-Pacific region.* SpringerLink. Retrieved from https://link.springer.com/content/pdf/10.1007/s11356-021-17560-w.pdf?pdf=button

[2] Amziane, S., & Sonebi, M. (2016). *Overview on bio-based building material made with plant aggregate.* RILEM Technical Letters, 31-38

[3] Crawford, R. H. (2022). *Greenhouse Gas Emissions of Global Construction Industries.* IOP Publishing Ltd. Retrieved September 6, 2022, form https://iopscience.iop.org/ article/10.1088 /1757-899X/1218/1/012047/pdf

[4] Fennell, P., Driver, J., Bataille, C. & Davis, S. (2022, March 24). *Going net zero for cement and steel.* Nature. Retrieved September 13, 2022, from https://media.nature.com/original/magazine-assets/d41586-022-00758-4/d41586-022-00758-4.pdf

[5] Statistics Netherlands. (2022, June 15). *Greenhouse gas emissions 11 percent lower in Q1 2022.* Retrieved September 6, 2022, from https://www.cbs.nl/en-gb/news/2022/24/ greenhouse-gas-emissions-11-percent-lower-in-q1-2022

[6] Ministry of Infrastructure and Water Management. (2021, December 23). *Circular Dutch economy by 2050.* Circular economy | Government.nl. Retrieved September 13, 2022, from https://www.government.nl/topics/circular-economy/circular-dutch-economy-by-2050

[7] *Sustainability of biobased materials in a circular economy* (n.d.). Retrieved September 12, 2022, from https://www.maastrichtuniversity.nl/research/sustainability-of-biobased-materials-circular-economy

[8] Habraken, A. (2021). Lecture material Resource Efficient Structural Engineering and Design 7PP5M0. The Netherlands, Eindhoven.

[9] Christie, J., Bodea, S., Solly, J., Menges, A. & Knippers, J. [THINkSHELL]. (2021, 30 april). *13: Filigree Shell Slabs - Christie et al* [Video]. YouTube. Retrieved September 15, 2022, from https://www.youtube.com/watch?v=Eyc1Ag98l7Q

[10] Beukers, A. & Hinte, V. E. (2013, April 30). *Lightness: The Inevitable Renaissance Minimum Energy Structures* (4th edition). nai010 publishers

[11] Vellaichamy, P., Kumarasamy, K., Navaneetha, S., & Veerasamy, S. (2019). *Buckling Analysis of columns.* IOSR Journal of Engineering. https://www.researchgate.net/publication/ 344584982_Buckling_Analysis_of_columns

[12] Chem Europe. (n.d.). *Buckling.* Retrieved February 28, 2023, from https://www.chemeurope.com/en/encyclopedia/Buckling.html#:~:text=In%20engineering%2C%20buckling%20is%20a,material%20is%20capable%20of%20withstanding.

[13] Pawlyn, M. (2016, October 6). *Biomimicry in Architecture* (2nd edition). RIBA Publishing.

[14] Zhang, D., Milanovic, N. R., Zhang, Y., Chu, P. K., & Miao, M. (2014). *Effects of humidity conditions fabrication on the interfacial shear strength of flax/unsaturated polyester composites.* Composites Part B-Engineering, 60, 186–192. https://doi.org/10.1016/j.compositesb.2013.12.031

[15] Sicomin Epoxy Systems. (2017). *SR InfuGreen 810: Green Epoxy systems for Injection and Infusion* (Version 01/03/2017) [Dataset]. Sicomin. Retrieved January 16, 2023, from http://sicomin.com/datasheets/product-pdf1167.pdf

[16] Karimah, A., Ridho, M. R., Munawar, S. S., Adi, D. S., Ismadi, Damayanti, R., Subiyanto, B., Fatriasari, W., & Fudholi, A. (2021, July 1). *A review on natural fibers for development of eco-friendly bio- composite: characteristics, and utilizations.* Journal of Materials Research and Technology; Elsevier BV. https://doi.org/10.1016/j.jmrt.2021.06.014

[17] Jawaid, M., Thariq, M., & Saba, N. (2019). *Mechanical and Physical Testing of Biocomposites, Fibre-Reinforced Composites and Hybrid Composites* (Woodhead Publishing Series in Composites Science and Engineering). Woodhead Publishing. https://doi.org/10.1016/C2016-0-04437-6

[18] Palaniswamy, N. & Mohamed, A. (2005). *Effect of single yarn twist and ply to single yarn twist ratio on strength and elongation of ply yarns.* Journal of Applied Polymer Science, 98, 2245-2252. doi:10.1002/app.22010

[19] Louer, L. (2022). *Optimization and Production of a Bio-based Bridge Railing through Robotic Filament Winding* [Master thesis]. Eindhoven: Eindhoven University of Technology.

[20] *Octopus*. (2023, February 13). Food4Rhino. https://www.food4rhino.com/en/app/octopus

[21] Wally. (2022). *Amine Blush - Composite Envisions.* Composite Envisions - Providing the Largest Selection of Composite Fabrics & Materials. Retrieved March 28, 2023, from https://compositeenvisions.com/document/amine-blush/